Available online at www.sciencedirect.com
SCIENCE DIRECT
Chemical Physics Letters 419 (2006) 390–393
CHEMICAL PHYSICS LETTERS
www.elsevier.com/locate/cplett

Self-assembled branched nanostructures of single-walled carbon nanotubes with DNA as linkers

Yanhong Lu, Xiaoying Yang, Yanfeng Ma, Feng Du, Zunfeng Liu, Yongsheng Chen *

Department of Chemistry, Key Laboratory for Functional Polymer Materials and Centre for Nanoscale Science and Technology, Institute of Polymer Chemistry, Nankai University, Weijin Road 94, Tianjin 300071, China

Received 3 November 2005; in final form 29 November 2005
Available online 27 December 2005

Abstract

Self-assembly of DNA functionalized single-walled carbon nanotubes is studied and atomic force microscopy images show that the highly branched structures were formed for the DNA functionalized SWNTs. The formation of the branched structures can be explained by the hybridization of DNA attached to the ends and sides of SWNTs based on the DNA complementary sequence-specific pairing interactions. Statistical analysis shows that the interconnected degree of self-assembled SWNTs via DNA hybridization is seven times more than that of single strand DNA functionalized SWNTs, which can only have the non-complementary interaction.

1. Introduction

Due to their unique electronic and structural characteristics [1–3], carbon nanotubes (CNTs) have emerged as important materials for nanofabrication in both electronic devices and sensors for a wide range of potential applications [4,5]. One key issue to materialize the full potential of CNTs is the need to assembly the CNTs, as building blocks, in predetermined patterns [6,7]. Though it is still a great challenge to efficiently organize CNTs as building blocks into multifunctional nanostructures and nanodevices, many progresses have been made for the nanofabrication using CNTs as building blocks for nano/micro devices or structures [8–11]. Recently, Woolley et al. [12] prepared aligned nanowires from the DNA-peptide-assisted assembly of CNTs on the surface of Si. Musselman et al. [13,14] obtained the morphologies of the form of Y-, X- and intra-loop junctions by peptide assistant assembly of SWNTs. Dai et al. [15] observed multicomponent structures through DNA-directed self-assembling of multiple carbon nanotubes and gold nanoparticles. Kotov et al. [16] obtained aligned SWNTs and robust SWNTs-polymer using a fusion method of SWNTs combing and layer-by-layer assembly. In this study, we obtained the branched structures through the self-assembly of DNA-attached SWNTs using the hybridization of two complementary single-strand DNA (ssDNA) chains attached on SWNTs. The formation of the branched structures may be attributed to the hybridization of DNA attached to the ends and sides of SWNTs based on the DNA sequence-specific pairing interactions. Statistical analysis shows that the interconnected degree (ID) of self-assembled SWNTs via DNA hybridization is seven times more than that of single strand DNA functionalized SWNTs.

2. Experimental

In a typical experiment, SWNTs, grown from our arc discharge method [17], were purified and shortened using previously published method [18]. The resultant purified and shortened SWNTs were re-dissolved in 5 mL 0.2% Triton X-100 suspension for chemical bonding with amino-end-functionalized ssDNA1 (i.e. [AmC6]ACGTAAAAAT-TACCATAAAT-5′) and its complimentary ssDNA2 chains (i.e. [AmC6]ATTTATGGTAATTTTTACGT-5′)

* Corresponding author. Fax: +86 22 23502749.
E-mail address: yschen99@nankai.edu.cn (Y. Chen).

0009-2614/$ - see front matter © 2005 Elsevier B.V. All rights reserved.
doi:10.1016/j.cplett.2005.11.116

(Shenggong Bioengineering Co. Ltd.), respectively, through the amide formation in the presence of *N*-(3-dimethyl aminopropyl)-*N*′-ethylcarbodiimide hydrochloride (EDC), *N*-hydroxysulfosuccinimide, sodium salt (NHS) and 2-morpholinoethanesulfonic acid monohydrate (MES) (Sigma–Aldrich) [19]. The samples were then centrifuged for 30 min at 14000 rpm (centrifuge: EPPENDORF, 5810 R). The upper supernatant were recovered and continued to centrifuge for 40 min at 14000 rpm. Then, the upper supernatant were recovered again and continued to centrifuge for another 5 h at 14000 rpm. The sediments were washed with double distilled water and 2X SSPE/0.2% SDS buffer (consisting of 2.5 mM EDTA, 7 mM sodium dodecyl sulfate, 300 mM NaCl, and 20 mM NaH_2PO_4 with pH 7.4) (Shenggong Bioengineering Co. Ltd.) by several centrifugation cycles at 14000 rpm in order to remove nonspecifically adsorbed DNA [20]. The samples (ca. 0.5 mg) were dispersed in 400 μL double distilled water finally. The two solutions of SWNTs functionalized with ssDNA1 and ssDNA2 were clear, transparent, blackish and homogenous suspensions, which were designed ssDNA1-SWNTs and ssDNA2-SWNTs, respectively. Raman spectra (not shown) of the SWNTs before and after functionalized with ssDNA1 or ssDNA2 show that the tangential vibration mode of functionalized SWNTs shift downward from 1597 to 1589 cm^{-1}, which is consistent with others' finding for the functionalized SWNTs [21].

The hybridization of ssDNA1-SWNTs with ssDNA2-SWNTs water solutions was performed in a water bath at 37 °C for 2 h. The hybridized products were designed dsDNA (double-strand DNA)-SWNTs.

3. Results and discussion

The morphology of the self-assembled dsDNA-SWNTs was examined with an atomic force microscopy (AFM, Nanoscope IV, Digital Instruments, VEECO) in tapping mode, as shown in Fig. 1. The typical images shown in Fig. 1a–d indicate that dsDNA-SWNTs form well-defined branched structures. Whereas much looser and more random distributed structures were observed in the control experiments for the unfunctionalized SWNTs (Fig. 2a) and the ssDNA1-SWNTs or ssDNA2-SWNTs solution (Fig. 2b), which were carried out for the same self-assembling procedure for comparison. Clearly, without assistance of DNA, no similar structures appeared and the SWNTs distributed in a completely random pattern, as shown in Fig. 2a. The sectional and low degree of interconnections of ssDNA-SWNTs in Fig. 2b could be due to the non-complementary ssDNA-ssDNA van der Waals binding of ssDNA chains anchored on SWNTs reported earlier [13].

Furthermore, a height of 1.81 nm and a length of ca. 7 nm (Fig. 3a,b) at the junction of dsDNA-SWNTs from the AFM analysis are well consistent with the diameter and the length of the dsDNA chain, corresponding to the DNA we used [22]. These results strongly suggest that the branched structures in Fig. 1 are formed due to the hybridization of the two complementary DNA chains attached to SWNTs based on the DNA sequence-specific pairing interaction.

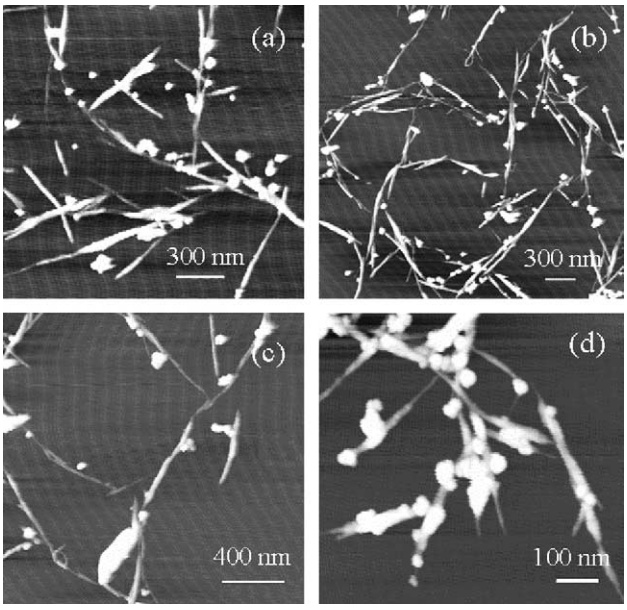

Fig. 1. AFM images of self-assembled SWNTs via hybridization of DNA, (a)–(d) are typical images from four different AFM samples.

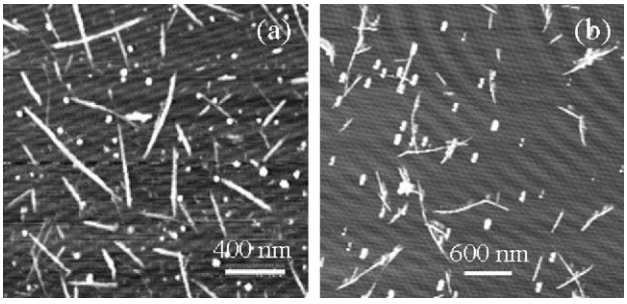

Fig. 2. Typical AFM images of unfunctionalized SWNTs (a) and ssDNA-SWNTs (b).

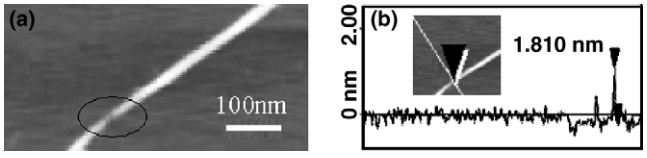

Fig. 3. A typical AFM image (a) for a DNA junction of dsDNA-SWNTs assembling. (b) is the AFM height cross-sectional analysis for the junction shown in the black circle in (a). AFM tip was scanned along the white thin line in inserted image (b). Black arrows in (b) indicate a height of 1.81 nm, corresponding to dsDNA diameter.

Thus, the formations of the branched structures of dsDNA-SWNTs could be illustrated in Scheme 1. SWNTs were oxidized with the nitric acid to introduce carboxylic groups at the ends and sides [18] for ssDNA grafting. The ssDNA1-attached SWNTs were then subjected to hybridize with the complementary DNA2 chains grafted on other SWNTs and form the branched structures.

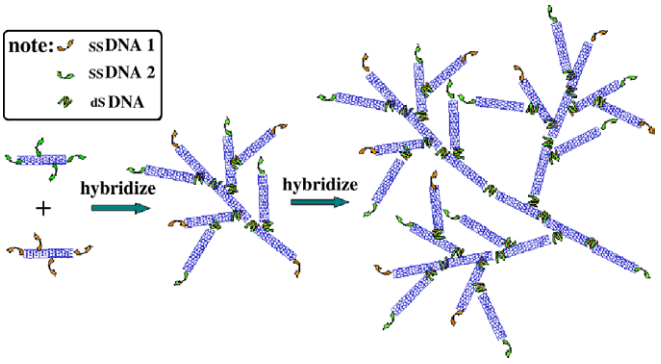

Scheme 1. Schematic representation of the formation process of the self-assembling of dsDNA-SWNTs.

To further support our findings of SWNTs assembly through DNA hybridization, a standard temperature DNA denaturizing experiment was carried for the dsDNA sample. Thus the dsDNA-SWNTs suspensions were boiled at 100 °C for 10 min [23] and then cooled immediately in an ice water bath to enable the dsDNA denatured. The AFM images show that the irregular forms of dsDNA-SWNTs after denaturation are quite similar to that of ssDNA functionalized SWNTs, as shown in Fig. 2b.

In order to describe the extent of self-assembly of SWNTs quantitatively, we also apply the following statistical analysis for the SWNTs before and after the assembling from the AFM images and use the interconnected degree (ID) to represent the extent of assembling (see below).

The average length $\bar{l}$ of the unfunctionalized SWNT (bundle) is calculated using Eq. (1).

$$\bar{l} = \frac{\sum_{i=1}^{n} l_i}{n}, \tag{1}$$

where l_i is the length of individual SWNT (bundle), n is the total number of unfunctionalized SWNTs in AFM images.

The total length of all the SWNTs (bundles) that connected together to form the number m interconnected structure in dsDNA-SWNTs can be calculated from the AFM images directly and is designed L_m, and the ID of this interconnected structure is designed ID_m, which can be calculated as

$$ID_m = \frac{L_m}{\bar{l}}. \tag{2}$$

Using Eq. (2), we can get the IDs for all the interconnected structures in the AFM images of dsDNA-SWNTs studied.

The overall average interconnected degree (designed as ID) of the dsDNA-SWNTs studied then can be calculated using

$$ID = \frac{\sum_{i=1}^{m} ID_i}{m}. \tag{3}$$

Similarly the ID of the unfunctionalized SWNTs, the ssDNA-SWNTs and the denatured dsDNA-SWNTs were calculated in the same way, respectively.

Table 1
Statistical analysis results of the ID of SWNTs using AFM images

SWNTs	Image area (μm^2)[a]	Interconnected degree
Unfunctionalized SWNTs	293.6	1
ssDNA-SWNTs	87.3	11
dsDNA-SWNTs	80.9	78
Denatured dsDNA-SWNTs	85.2	17

[a] 17 AFM images covering total 547 μm^2 area were used for the statistical analysis.

The statistical analysis results are identified in Table 1. The ID (78) for the dsDNA-SWNT with sequence-specific pairing DNA hybridization is over ~7 times of the ID (11) for the SWNTs without the DNA hybridization. The ID for the unfunctionalized SWNTs is normalized as 1 as the base for comparisons. More convincing results came from the denaturation studies. As seen from Table 1, after the denaturation, the ID of the dsDNA-SWNTs (78) decreases significantly to 17, which is close to the original ID of the ssDNA-SWNTs sample (11). We argue that this dramatic decrease of ID is because the DNA pairing junctions in the branched structures were destroyed due to the denaturation of the double strand DNA. This result clearly supports that the hybridization of the DNA attached to SWNTs plays a critical role for the assembly of SWNTs to form branched structures. The slightly higher ID (17) of denatured dsDNA-SWNTs than that ID (11) of the ssDNA-SWNTs indicates that not all the pairing of dsDNA was destroyed.

In conclusion, the self-assembled branched structures of SWNTs could be formed with single-strand DNA functionalization. Comparing with the control experiments, we believe that such a self-assembling behavior could be attributed to the sequence-specific pairing DNA hybridization. This DNA-assisted assembling of SWNTs could offer a potential method to facilitate the construction of the desired nanoscale multicomponent/multifunctional architectures of SWNTs for various electrical and molecular sensing applications. Further experiments are underway to investigate the interactions among SWNTs in the self-assembled structures.

Acknowledgments

This work was supported by the '863' project (Grant No. 2003AA302640) of Ministry of Science and Technology of China, Postdoctoral Funding (Grant No. 20040055020) of Ministry of Education of China and NSF Funding (Grant No. 043803711) of Tianjin City.

References

[1] T.W. Odom, J.L. Huang, P. Kim, C.M. Lieber, J. Phys. Chem. B 104 (2000) 2794.
[2] C.N.R. Rao, B.C. Satishkumar, A. Govindaraj, M. Nath, ChemPhysChem 2 (2001) 78.
[3] P. Avouris, Acc. Chem. Res. 35 (2002) 1026.

[4] K. Besteman, J. Lee, F.G.M. Wiertz, H.A. Heering, C. Dekker, NanoLetters 3 (2003) 727.
[5] I. Heller, J. Kong, H.A. Heering, K.A. Williams, S.G. Lemay, C. Dekker, NanoLetters 5 (2005) 137.
[6] J. Liu, M.J. Casavant, M. Cox, D.A. Walters, P. Boul, W. Lu, A.J. Rimberg, K.A. Smith, D.T. Colbert, R.E. Smalley, Chem. Phys. Lett. 303 (1999) 125.
[7] M. Senthil Kumar, T.H. Kim, S.H. Lee, S.M. Song, J.W. Yang, K.S. Nahm, E.-K. Suh, Chem. Phys. Lett. 383 (2004) 235.
[8] J. Kong, N.R. Franklin, C. Zhou, M.G. Chapline, S. Peng, K. Cho, H. Dai, Science 287 (2000) 622.
[9] A. Bachtold, P. Hadley, T. Nakanishi, C. Dekker, Science 294 (2001) 1317.
[10] V. Derycke, R. Martel, J. Appenzeller, Ph. Avouris, NanoLetters 1 (2001) 453.
[11] H.W.C. Postma, T. Teepen, Z. Yao, M. Grifoni, C. Dekker, Science 293 (2001) 76.
[12] H. Xin, A.T. Woolley, J. Am. Chem. Soc. 125 (2003) 8710.
[13] G.R. Dieckmann, A.B. Dalton, P.A. Johnson, J. Razal, J. Chen, G.M. Giordano, E. Muñoz, I.H. Musselman, R.H. Baughman, R.K. Draper, J. Am. Chem. Soc. 125 (2003) 1770.
[14] V. Zorbas, A. Ortiz-Acevedo, A.B. Dalton, M.M. Yoshida, G.R. Dieckmann, R.K. Draper, R.H. Baughman, M. Jose-Yacaman, I.H. Musselman, J. Am. Chem. Soc. 126 (2004) 7222.
[15] S. Li, P. He, J. Dong, Z. Guo, L. Dai, J. Am. Chem. Soc. 127 (2005) 14.
[16] B.S. Shim, N.A. Kotov, Langmuir 21 (2005) 9831.
[17] X. Lv, F. Du, Y. Ma, Q. Wu, Y. Chen, Carbon 43 (2005) 2020.
[18] J. Liu, A.G. Rinzler, H. Dai, J.H. Hafner, R.K. Bradley, P.J. Boul, A. Lu, T. Iverson, K. Shelimov, C.B. Huffman, F. Rodriguez-Macias, Y. Shon, T.R. Lee, D.T. Colbert, R.E. Smalley, Science 280 (1998) 1253.
[19] M. Hazani, R. Naaman, F. Hennrich, M.M. Kappes, NanoLetters 3 (2003) 153.
[20] S.E. Baker, W. Cai, T.L. Lasseter, K.P. Weidkamp, R.J. Hamers, NanoLetters 2 (2002) 1413.
[21] P.W. Chiu, G.S. Duesberg, U. Dettlaff-Weglikowska, S. Roth, Appl. Phys. Lett. 80 (2002) 3811.
[22] A. Anne, A. Bouchardon, J. Moirous, J. Am. Chem. Soc. 125 (2003) 1112.
[23] S.J. Byrne, S.A. Corr, Y.K. Gun'ko, J.M. Kelly, D.F. Brougham, S. Ghosh, Chem. Commun. (2004) 2560.